Section 0.1.1 Introduction to TEM/STEM

FIGURE 1.1. The electron microscope built by Ruska (in the lab coat) and Knoll, in Berlin in the early 1930s.

Transmission Electron Microscopy, A textbook for Materials Science, David B Williams and C Barry Carter, Springer, 2nd edition 2009

NSF
2519465
2519466
2519467
THE UNIVERSITY of NORTH CAROLINA at CHAPEL HILL
UNIVERSITY OF MARYLAND
USC University of Southern California

CITEAM

Evolution of TEMs

FIGURE 1.9. (Continued)

12 .... The Transmission Electron Microscope

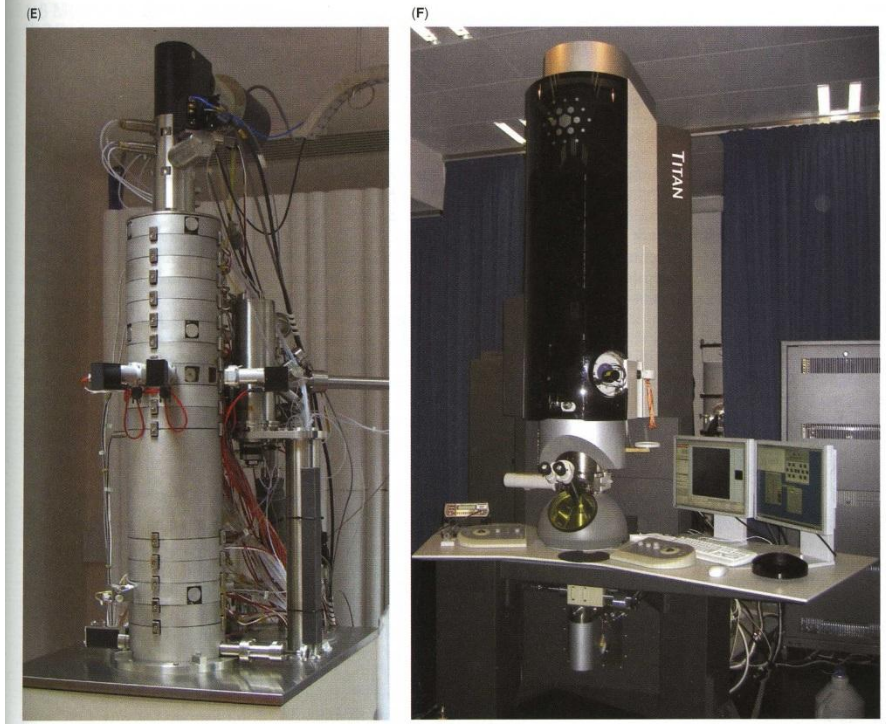

FIGURE 1.9. A selection of different commercial TEMs: (A) JEM 1.25 MeV HVEM. Note the size of the instrument; often the high-voltage tank is in another room above the column. (B) Zeiss HRTEM with a C_s corrector and an in-column energy filter. Note the large frame to provide high mechanical stability for the highest-resolution performance. (C) Hitachi 200 keV dedicated STEM; note the absence of a viewing chamber. Such instruments are often designed to aid failure analysis for the semiconductor device manufacturers. Specimens thinned from wafers on the production line can be easily transferred and examined. (D) JEOL 200 keV TEM/STEM; note also the absence of a viewing chamber. (E) Nion 200 keV ultrahigh vacuum SuperSTEM; the only US-manufactured (S)TEM and current holder of the world record image resolution (F) FEI Titan. Comparison with Ruska's instrument (Figure 1.1), which is 70–80 years older than these instruments, is instructive.

Transmission Electron Microscopy, A textbook for Materials Science, David B Williams and C Barry Carter, Springer, 2nd edition 2009

CITEAM

Cross section of the JEOL 2100F TEM

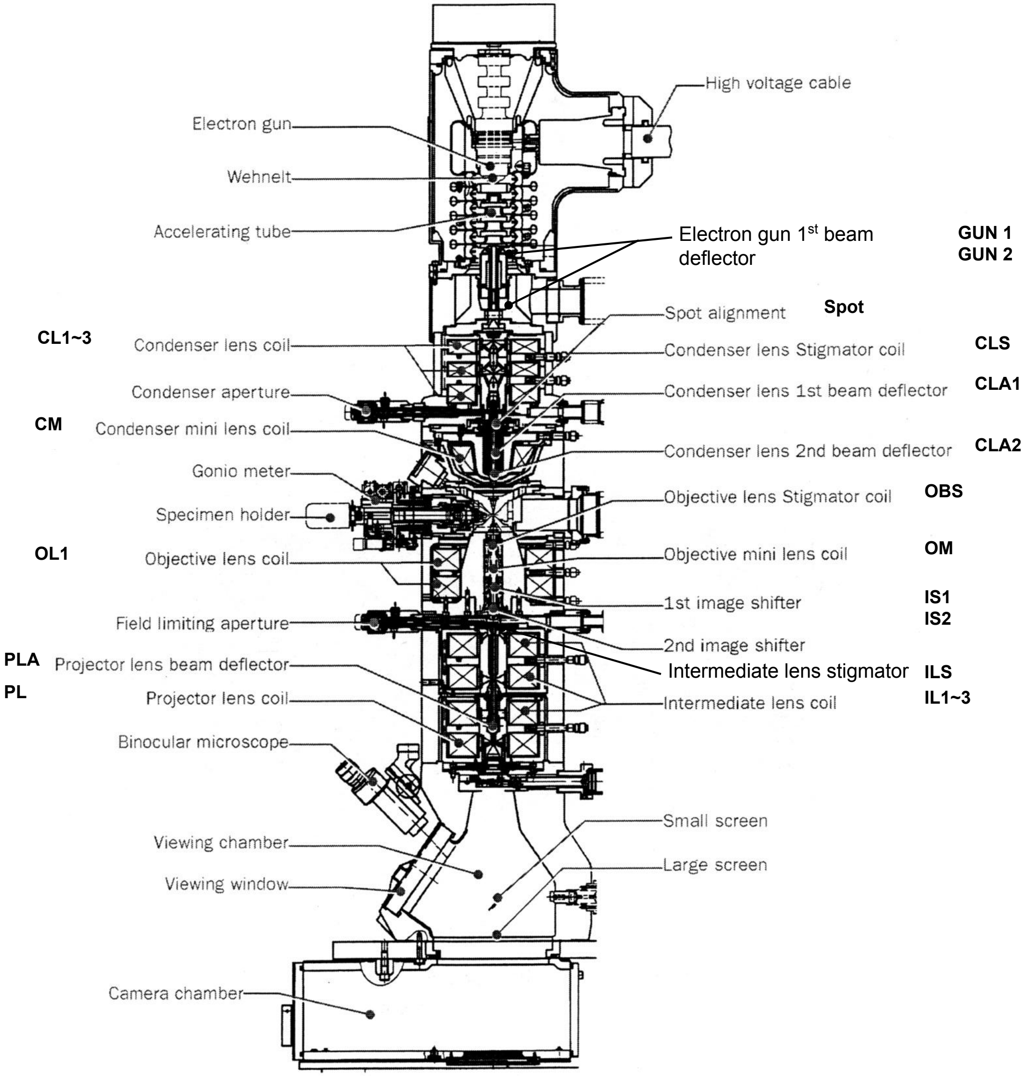

https://www.nanocenter.umd.edu/aimlab/equipment/detail.php?id=sc144ef1db89bbfc

NEOARM Highlights

NEOARM 200 F Cs corrected TEM in the IDEA Factory

- High Brightness Cold FEG
- 30-200kV
- HR Pole Piece for maximum flexibility between analytical and resolution optimization
- IDES Technology integration
- Dual, large-area SDDs for efficient EDS collection
- Highly stable probe current
- COSMO Automated Corrector alignments

Cross section of NEOARM Column

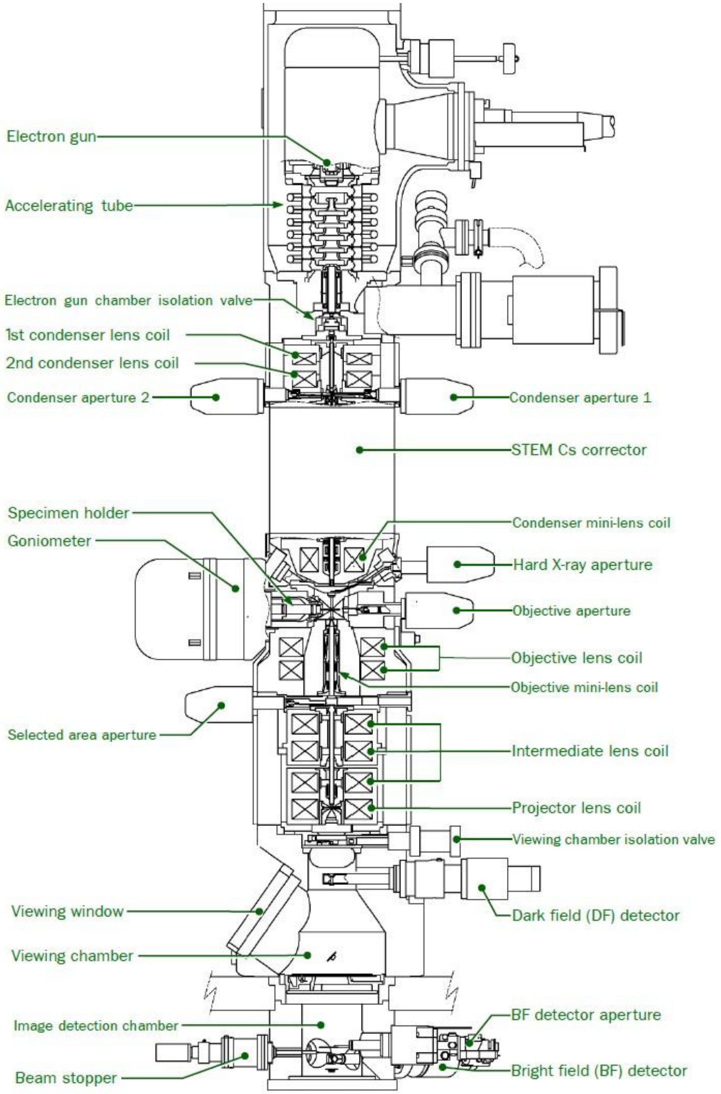

Figure 3.3 Cross section of column

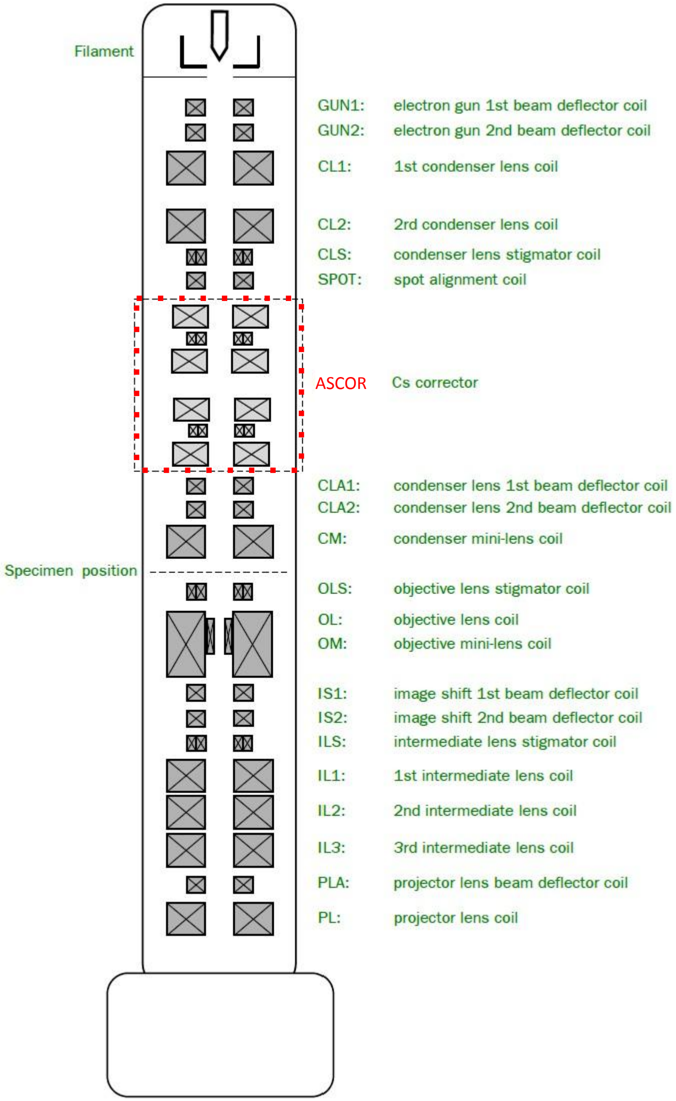

Figure 3.4 Location of coils and lenses

From JEOL

Electron beam sample interaction

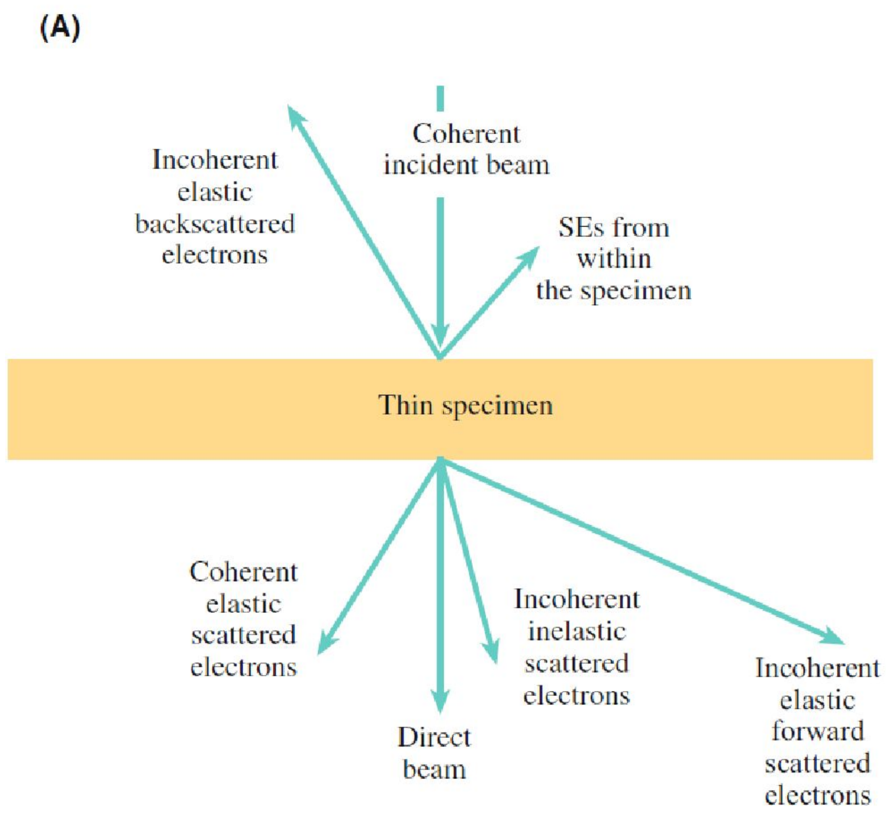

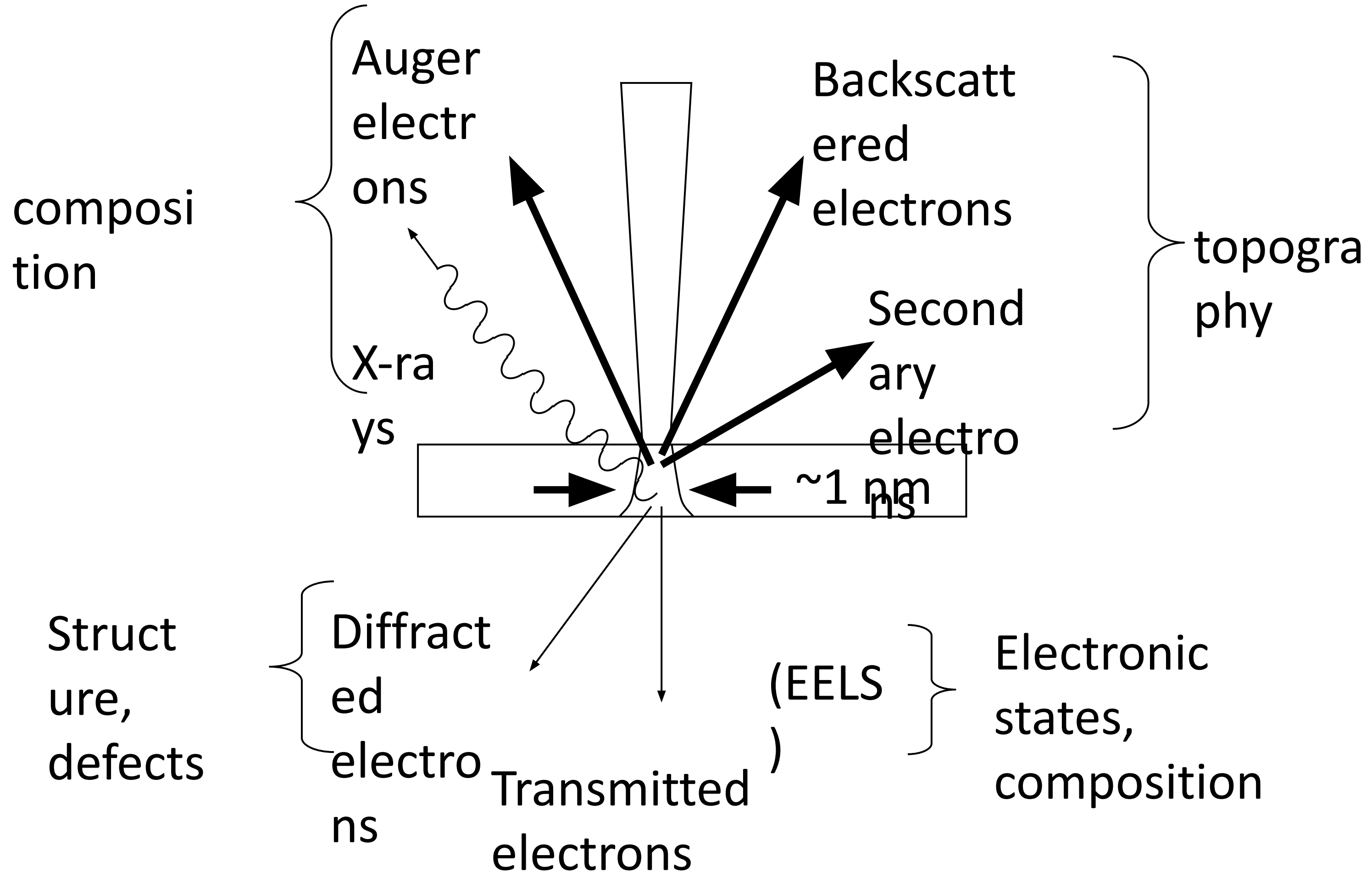

Transmission Electron Microscopy, A textbook for Materials Science, David B Williams and C Barry Carter, Springer, 2nd edition 2009

Imaging and Diffraction in TEM

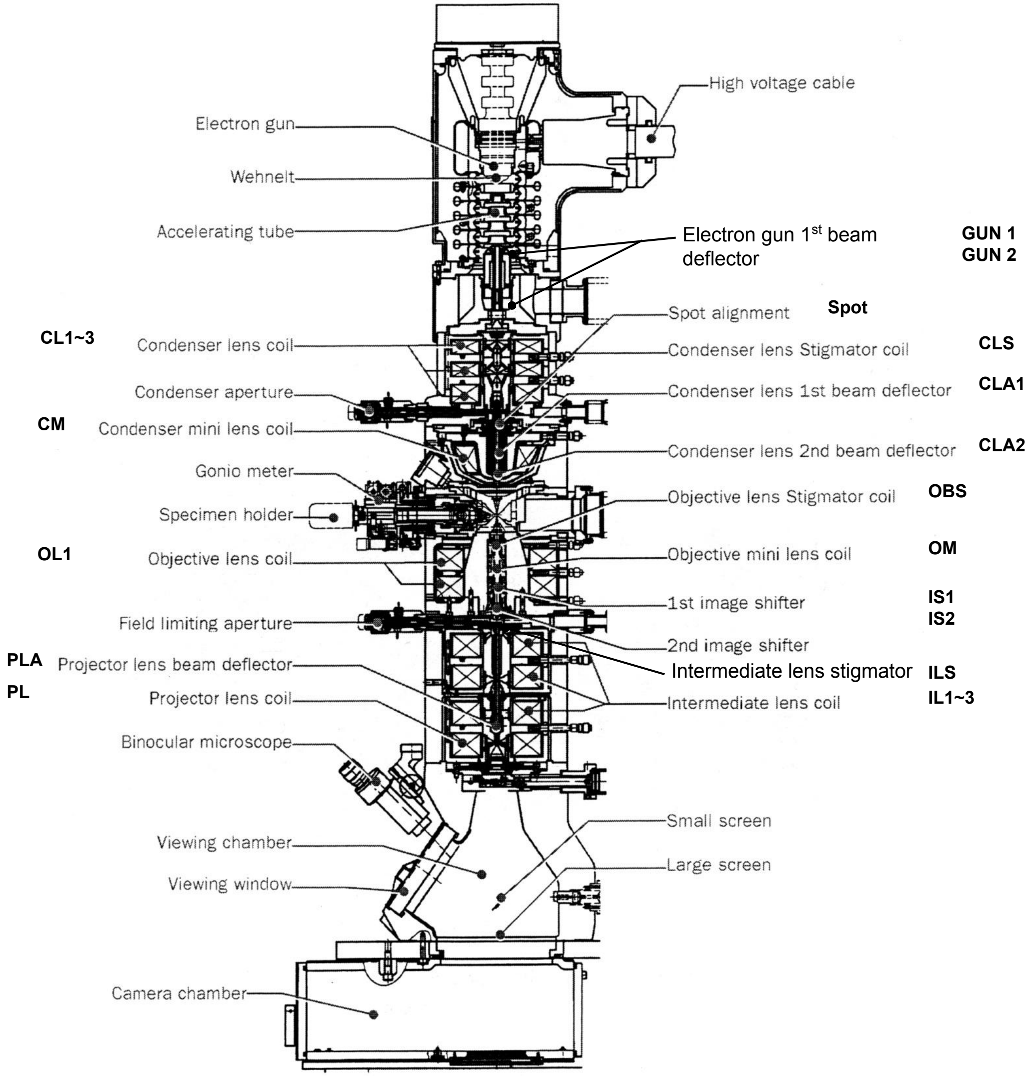

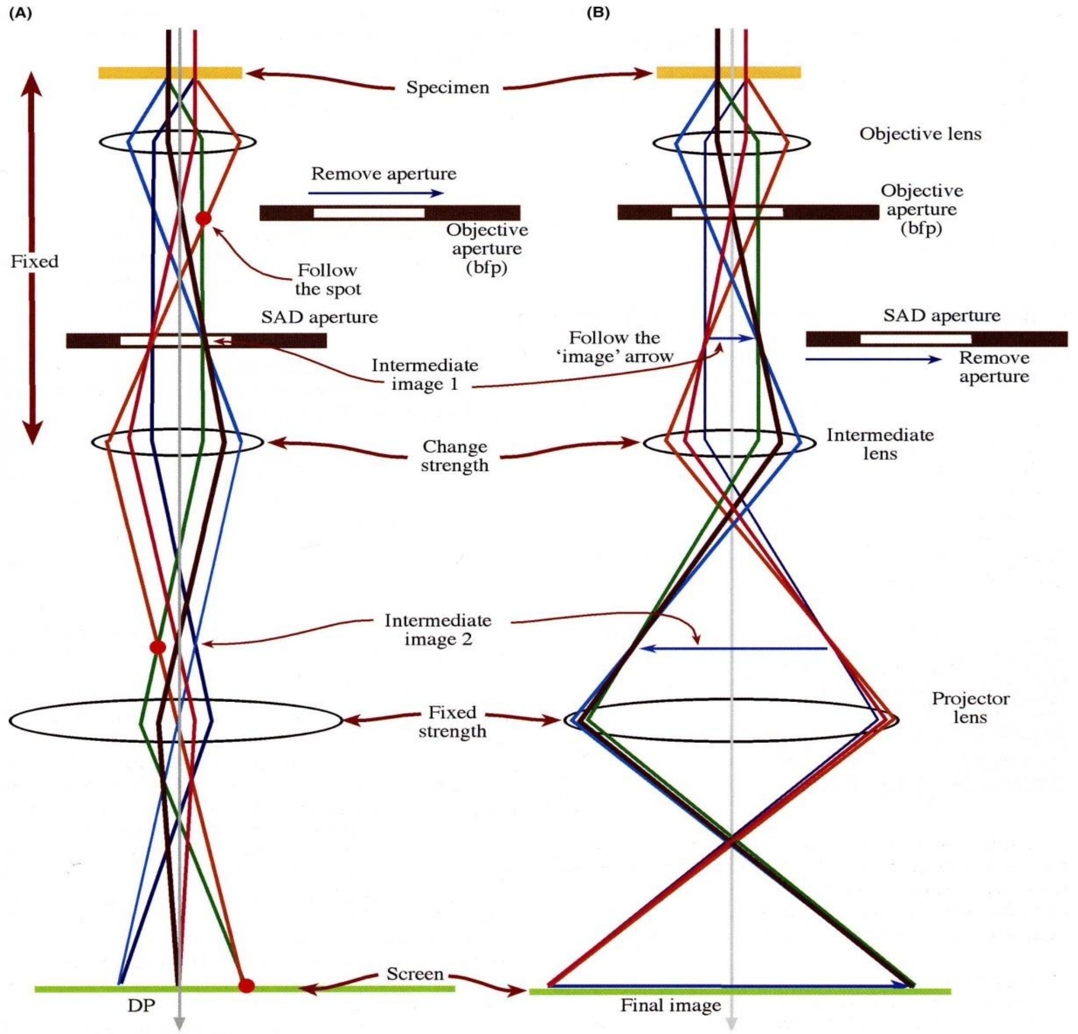

FIGURE 9.12. The two basic operations of the TEM imaging system involve (A) diffraction mode: projecting the DP onto the viewing screen and (B) image mode: projecting the image onto the screen. In each case the intermediate lens selects either the BFP (A) or the image plane (B) of the objective lens as its object. The imaging systems shown here are highly simplified. Most TEMs have many more imaging lenses, which give greater flexibility in terms of magnification and focusing range for both images and DPs. The SAD and objective diaphragms are also shown appropriately inserted or retracted. NOTE: This is a highly simplified diagram showing only three lenses. Modern TEM columns have many more lenses in their imaging systems.

Transmission Electron Microscopy, A textbook for Materials Science, David B Williams and C Barry Carter, Springer, 2nd ed. 2009

Bright Field and Dark Field in TEM

Bright Field

Dark Field

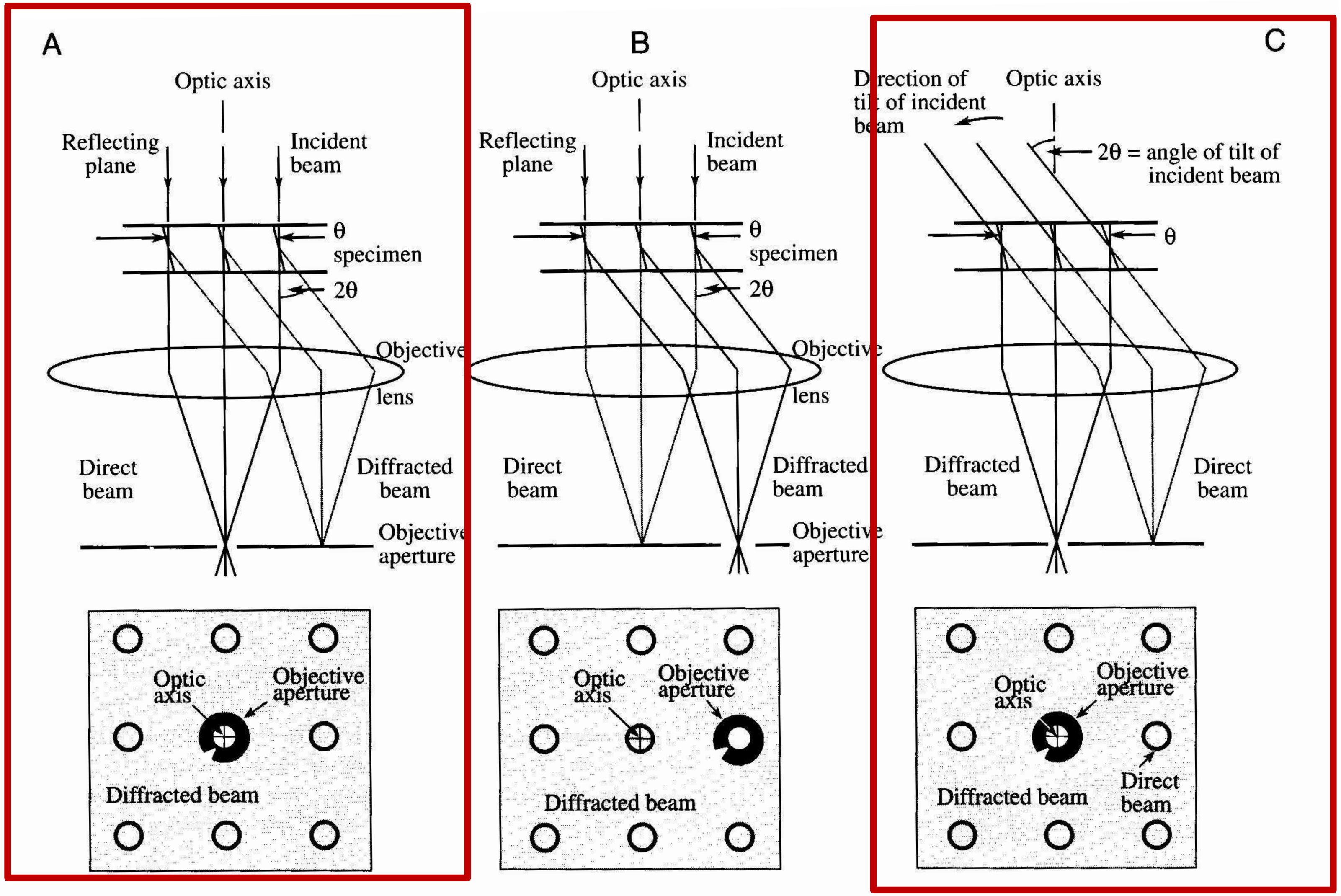

Figure 9.14. Ray diagrams showing how the objective lens/aperture are used in combination to produce (A) a BF image formed from the direct beam, (B) a displaced-aperture DF image formed with a specific off-axis scattered beam, and (C) a CDF image where the incident beam is tilted so that the scattered beam remains on axis. The area selected by the objective aperture, as seen on the viewing screen, is shown below each ray diagram.

Transmission Electron Microscopy, A textbook for Materials Science, David B Williams and C Barry Carter, Springer, 2nd edition 2009

STEM imaging

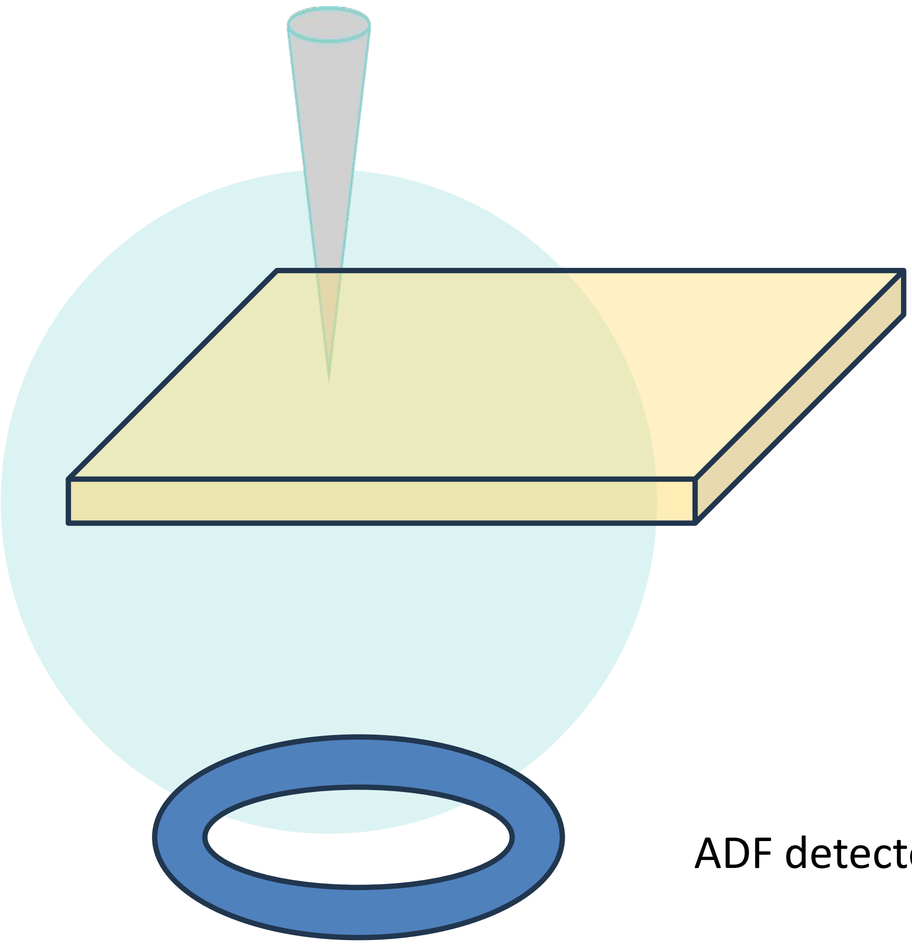

ADF detector

In STEM mode the electron beam is scanned on an area of the sample and the selected detector collects the signal from each point

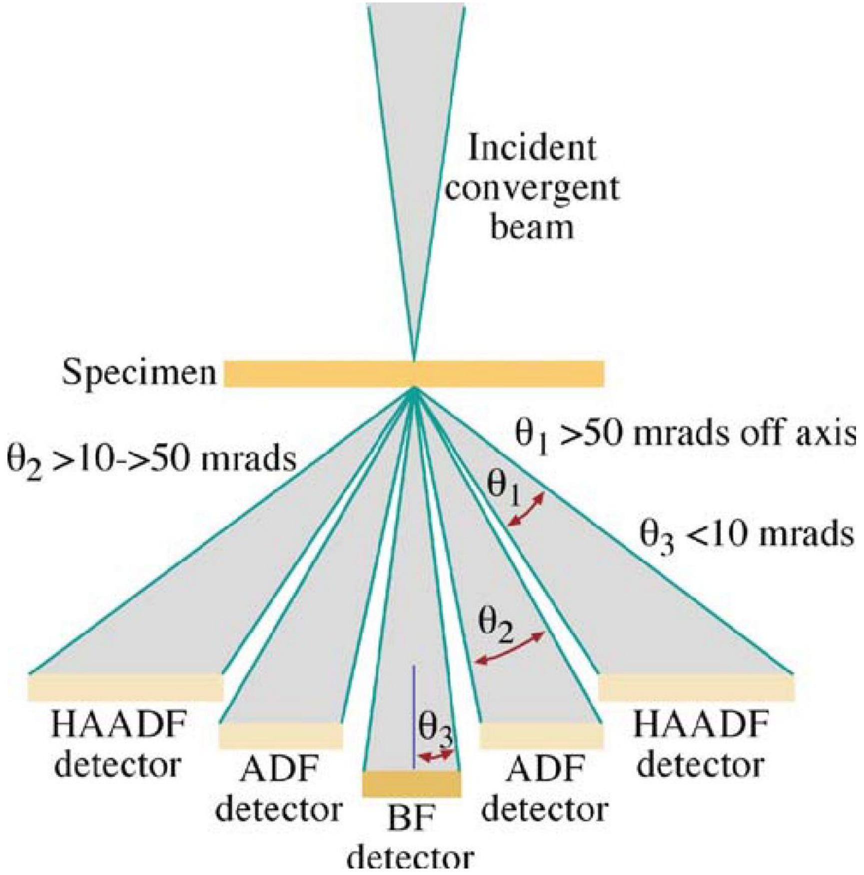

BF Bright Field detector
ADF Annular Dark Field detector
HAADF High Angle Annular Dark Field detector

Transmission Electron Microscopy, David Williams and Barry Carter, 2nd ed. (2009)

NEOARM Specifics for STEM Imaging

STEM Imaging Modes

- High-angle annular dark field (HAADF)
- Bright field (BF)
- Annular bright field (ABF)

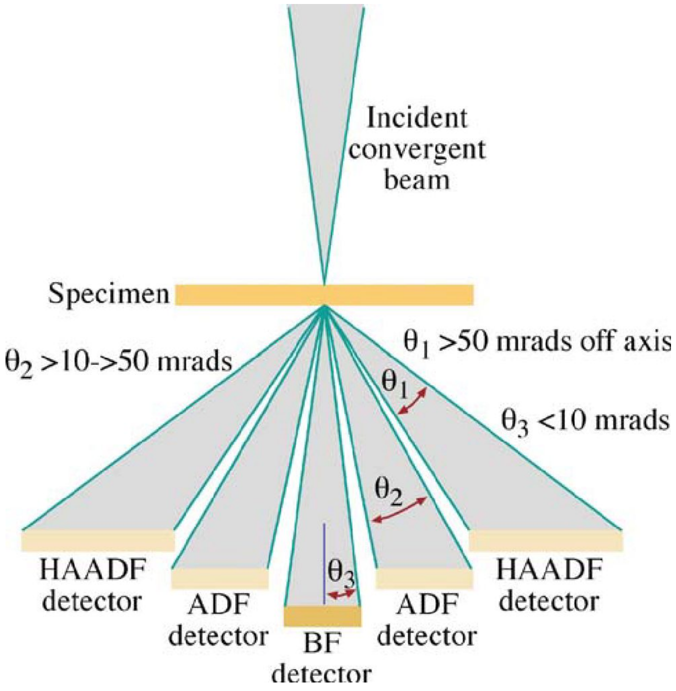

Transmission Electron Microscopy, David Williams and Barry Carter, 2nd ed. (2009)

Diffraction Pattern (STEM)

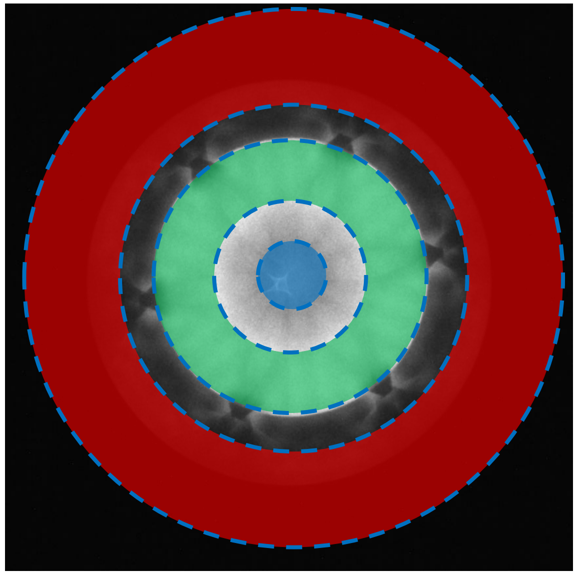

HAADF:

Z-contrast

Robust, easy to understand

BF:

Close to conventional TEM

Phase Contrast (not straightforward)

ABF:

Enhanced contrast for light elements

Robust, easy to understand

$SrTiO_3$ Example

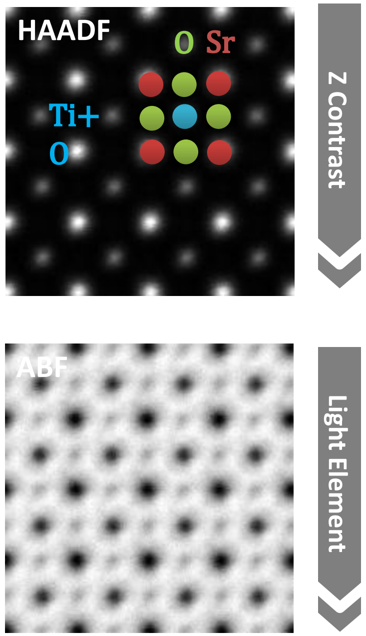

From JEOL

NEOARM Specifics

NEOARM
- High-brightness Cold Field-Emission Gun
- Column and Corrector alignments provided at 30 kV, 80 kV, 200 kV
- Resolution of .23nm in TEM
- +/- 35/30 degrees of tilt in X/Y

STEM C_s-Corrector
- CEOS ASCOR – Second-generation, higher-order corrector
- Enables high-resolution imaging with large convergence angles and high probe currents
- JEOL COSMO automated Corrector alignment routine

HAADF STEM Image

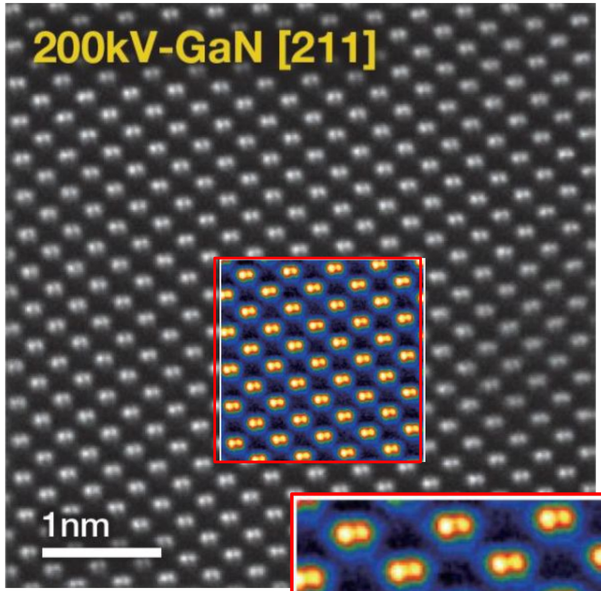

FFT

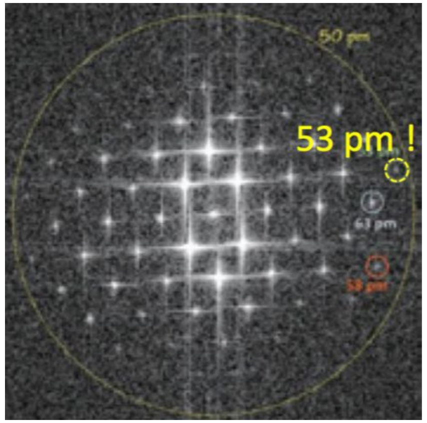

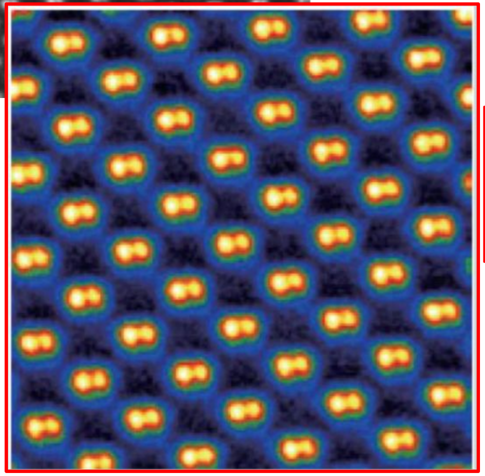

Ga-Ga dumbbells split by 63 pm

From JEOL

JEOL NEOARM + CEFID Configuration

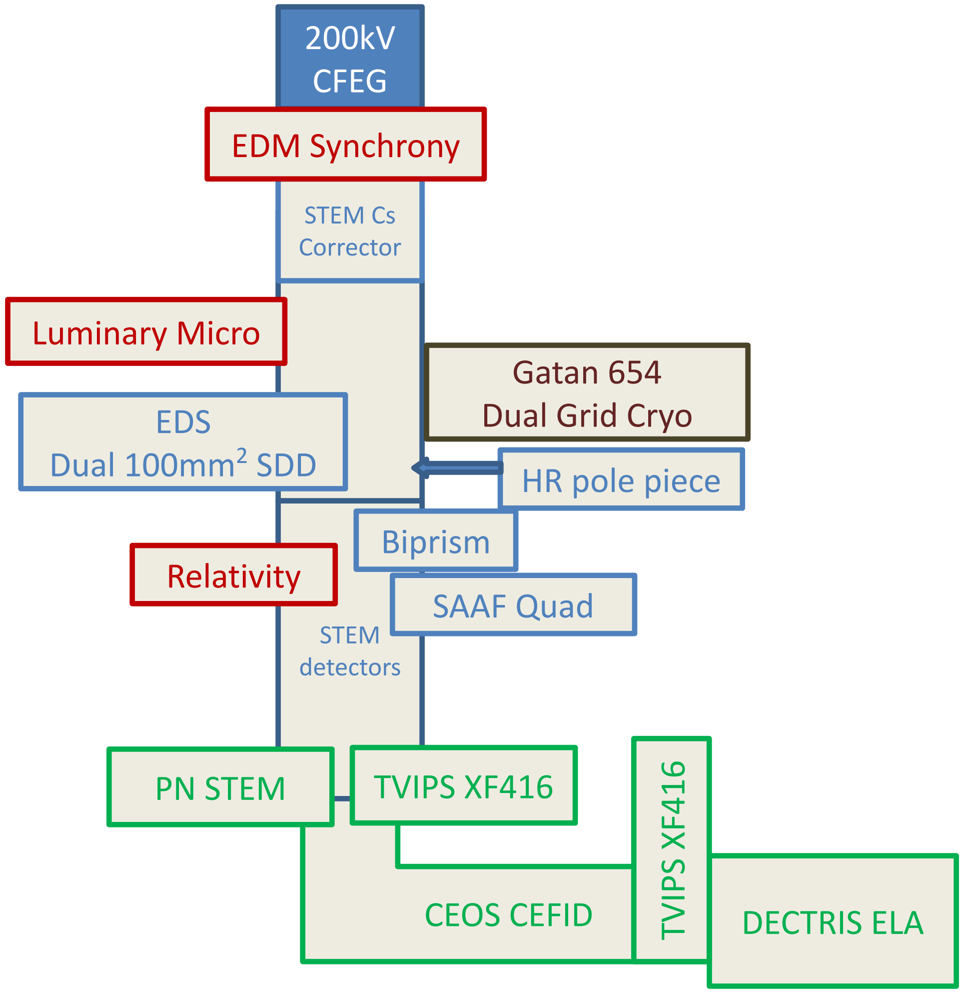

From JEOL

JEOL

- *STEM C_s-Corrected --Aligned at 30kV, 80kV, 200kV*
- *Dual EDS*
- *STEM HAADF, STEM ABF detectors*
- *Segmented STEM (SAAF) Quad Detector*
- *STEM Lorentz & NBD alignments*
- *Biprism*
- *PyJEM (Python-based) scripting control of JEOL + IDES*

IDES

- *EDM Synchrony (Electrostatic Dose Modulator)*
- *Luminary Micro*
- *Relativity Sub-framing*

CEOS/TVIPS/DECTRIS/PN Detector

- *CEFID energy filter*
  - *ELA detector*
  - *TVIPS XF416 detector*
- *TVIPS XF416 Bottom mount*
  - *Use with IDES Relativity*
- *PN Detector for STEM*

Other

- *Gatan Straining Holder (654)*
- *Simple Origin Dual Grid Cryo*
- *Protochips Poseidon holder*
- *Protochips Atmosphere holder*
- *Protochips Fusion holder*

Sample 1 to be Analyzed

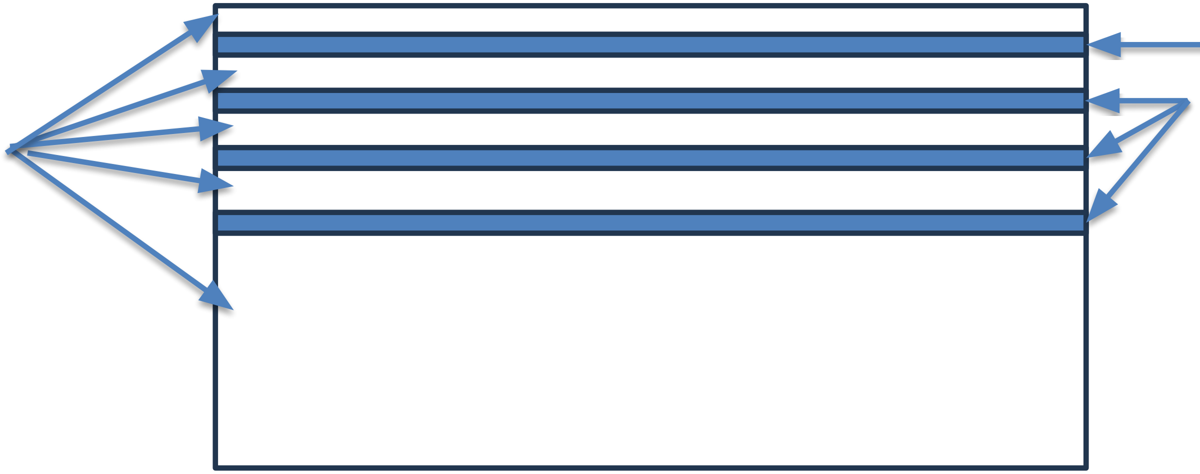

Sample from Riss Card at UMD

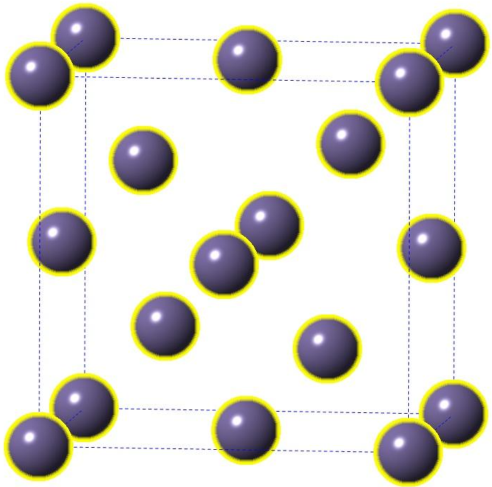

Ge

a=0.5658 nm

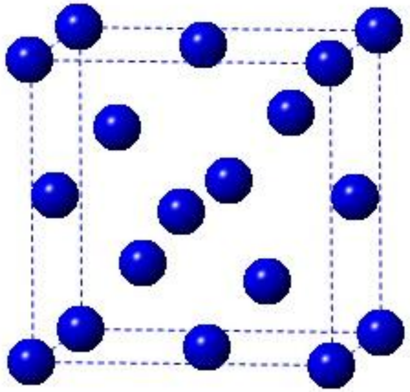

Si

a=0.543 nm

Ge and Si are in group IV of the periodic table. However, Ge is heavier than Si and has larger lattice constant. The contrast between the $Si_{1-x}Ge_x$ layers and pure Si layers depends on x. ADF in STEM gives higher contrast because of the larger atomic mass of Ge compared to Si.

What to look for:

Thickness of SiGe layers

Sharpness of the Si/SiGe interfaces

Defects in the multilayer

Misfit Dislocations

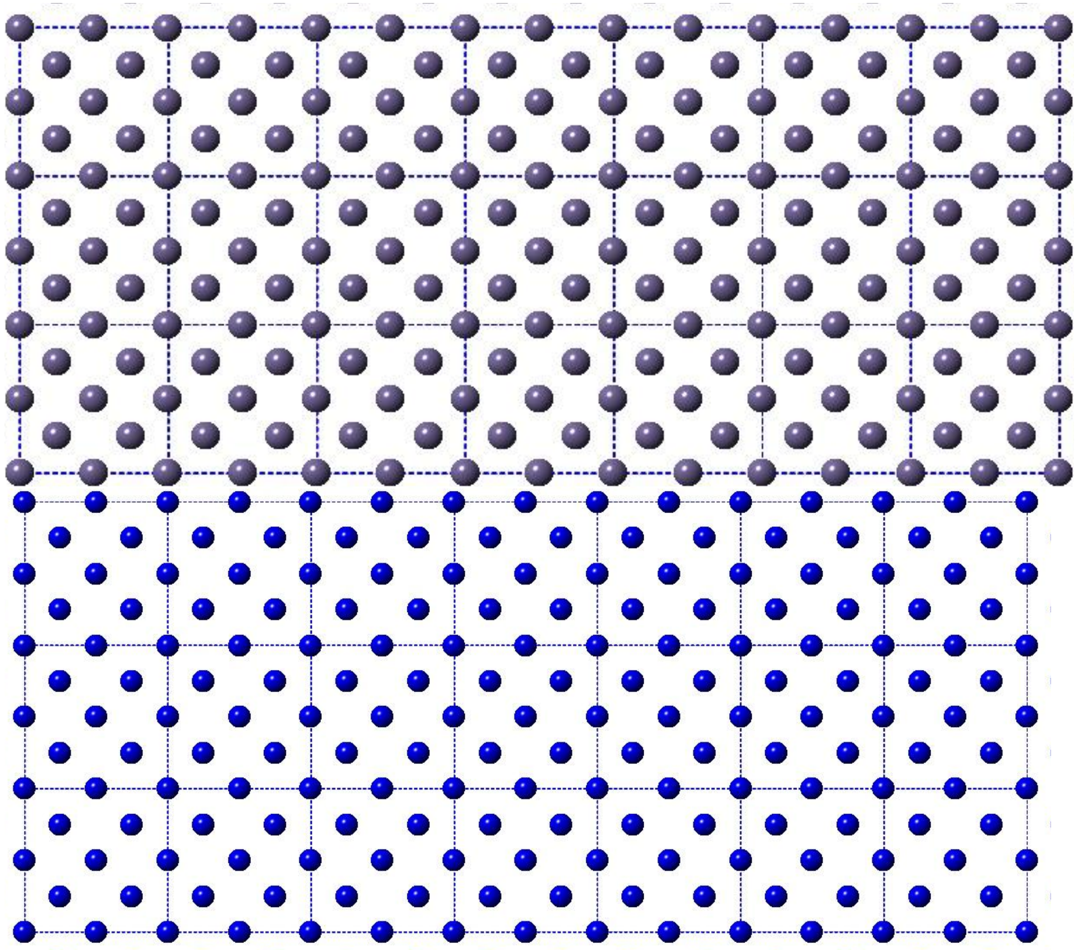

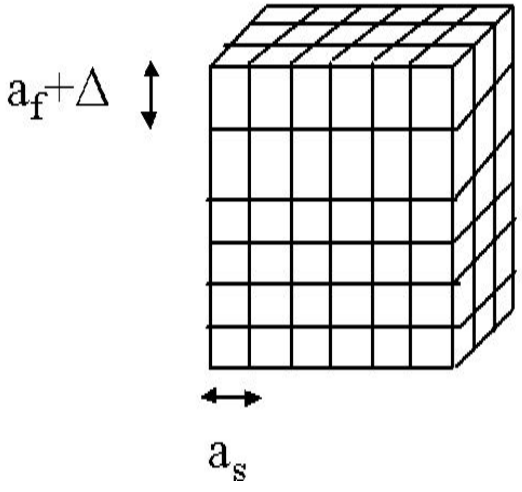

Film under strain

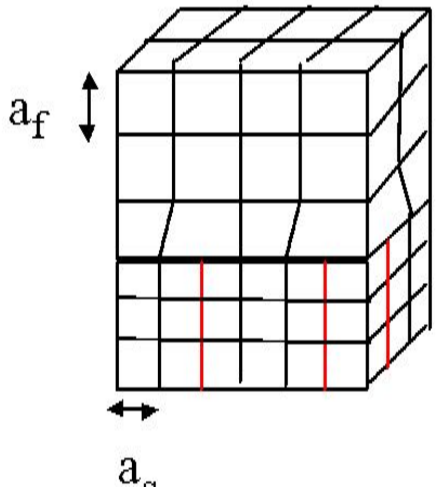

Partially relaxed film

Misfit dislocations (red) form at the interface between film and substrate. Dislocations degrade the properties of the sample.

CITEAM

Sample 2 : $TbFeO_3$ on YSZ

- Used for photocatalysis, electronics, and magnetic applications.
- $TbFeO_3$ film deposited by PLD on Y_2O_3 stabilized zirconia Zr_2O_4 with hexagonal structure.
- $Y_xZr_{1-x}O_3$ the value of x determines the crystal structure of YSZ and this controls the crystal structure of $TbFeO_3$ and its properties

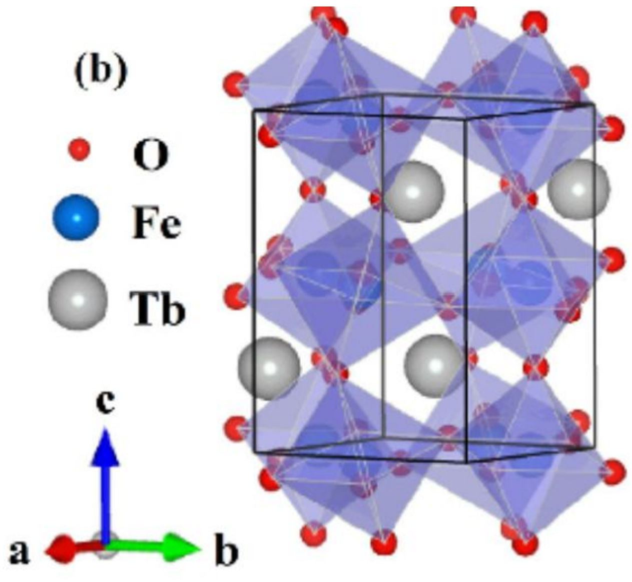

Usual structure Orthorhombic

It is known that under special deposition/synthesis conditions, $TbFeO_3$ grows in a hexagonal structure, which has a completely different property compared to the orthorhombic one. Using autonomous deposition condition optimization experiment Dr. Takeuchi's team found the best condition to fabricate phase pure metastable hexagonal phase, and this is what we show here.

This structure could also have defects that affect the properties.

Cao, Yiming et. Al. (2016). Magnetic phase transition and giant anisotropic magnetic entropy change in TbFeO3 single crystal. Journal of Applied Physics. 119. 063904. 10.1063/1.4941105.

Antiphase Domain Boundaries In Ba(Sr) TiO_3

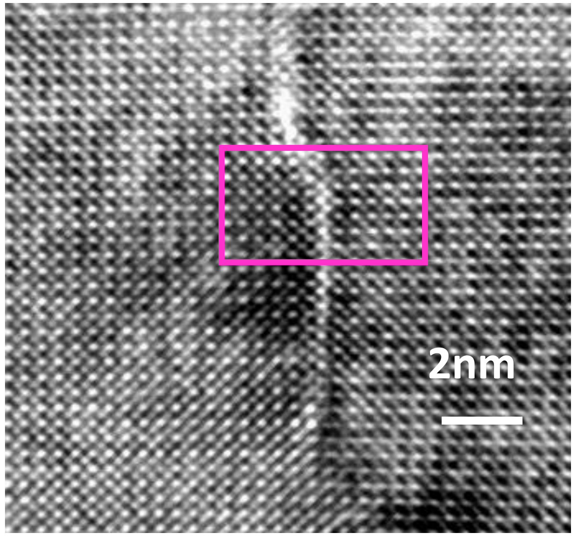

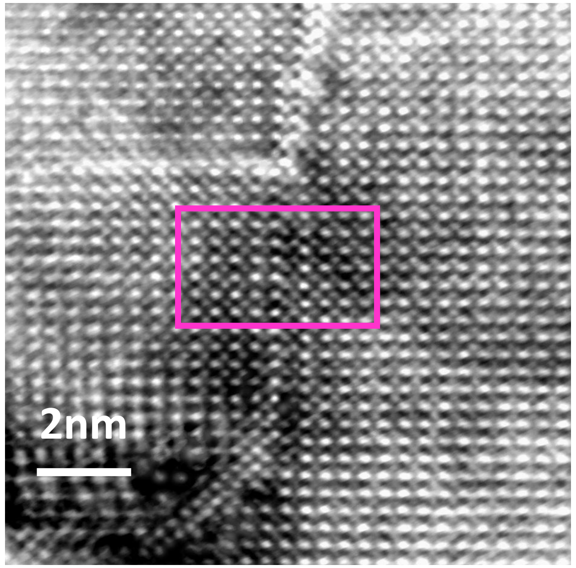

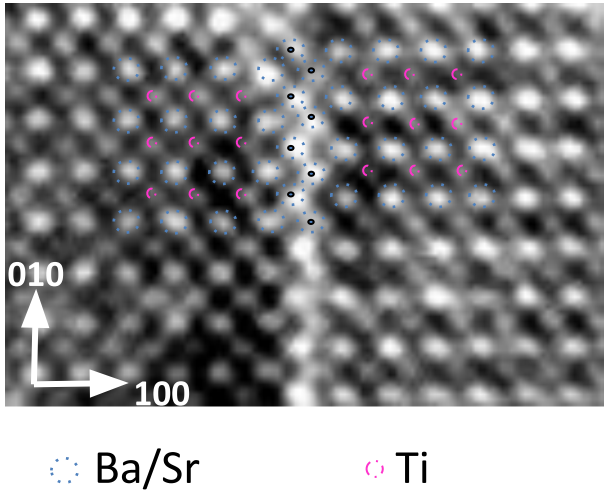

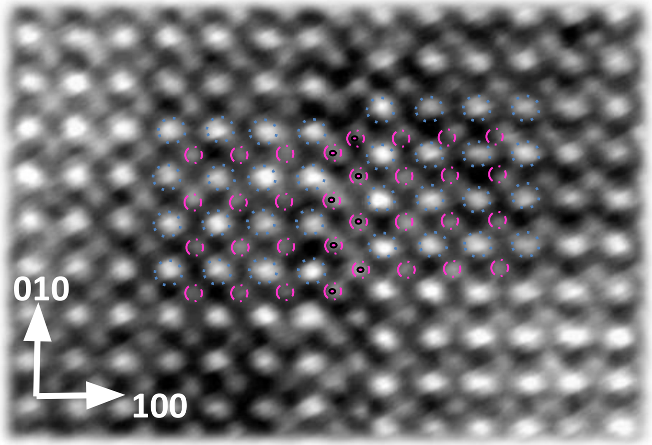

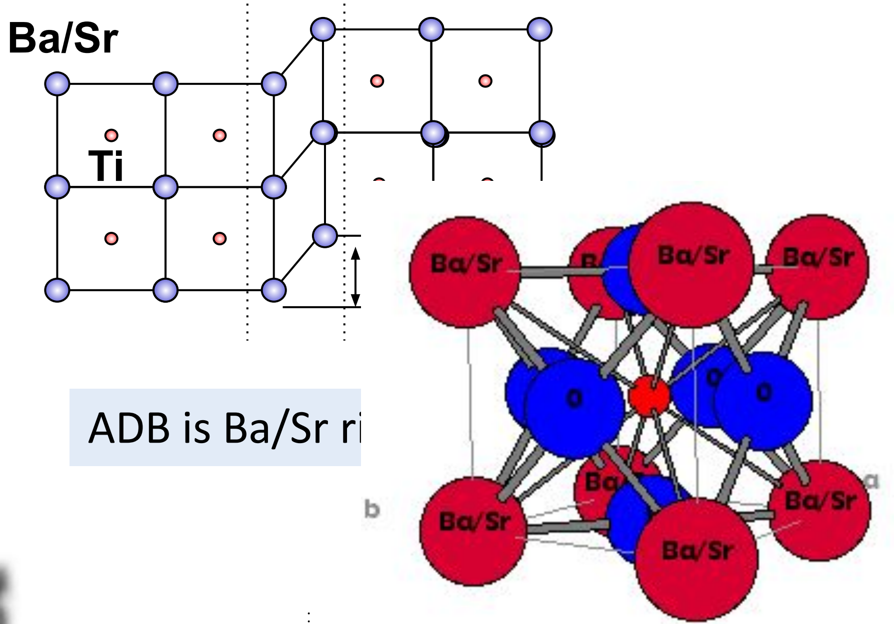

ADB is Ba/Sr ri

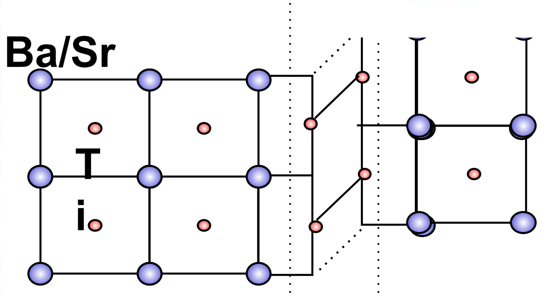

ADB is Ti rich

H. Zheng, L. Salamanca-Riba, R. Ramesh, and H. Li, Appl. Phys. Lett. **85**, 2905-7 (2004).